

DOI: 10.24850/j-tyca-14-05-08

Articles

Estimation of the vegetal cover fraction in corn from information obtained with remote sensing

Estimación de la fracción de cobertura vegetal en maíz a partir de información obtenida con sensores remotos

José M. Muñoz¹, ORCID: <https://orcid.org/0000-0003-2602-832X>

Martín A. Bolaños², ORCID: <https://orcid.org/0000-0002-8110-1051>

Enrique Palacios³, ORCID: <https://orcid.org/0000-0002-1716-9377>

Luis A. Palacios⁴, ORCID: <https://orcid.org/0000-0001-7963-7319>

José M. Salvador⁵, ORCID: <https://orcid.org/0000-0002-8814-9891>

¹Posgrado en Hidrociencias, Colegio de Postgraduados, Texcoco, Estado de México, México, jmiguel.muper@gmail.com

²Posgrado en Hidrociencias, Colegio de Postgraduados, Texcoco, Estado de México, México, bolanos@colpos.mx

³Posgrado en Hidrociencias, Colegio de Postgraduados, Texcoco, Estado de México, México, epalaciospave80@gmail.com

⁴Servicios de Estudios en Ingeniería y Sistemas, S.A. de C.V., Hermosillo, Sonora, México, luispalacios@seissa.com.mx



⁵Posgrado en Hidrociencias, Colegio de Postgraduados, Texcoco, Estado de México, México, sl_castillo990@gmail.com

Corresponding author: Martín A. Bolaños, bolanos@colpos.mx

Abstract

The Fractional vegetation cover (FVC) is a biophysical variable related to biomass, leaf area index, crop coefficient, among others. Currently, with the wide availability of satellite images, it is possible to estimate FVC extensively using vegetation indices (VI). However, it is essential to examine the relationship between VCF measured in the field and that estimated with satellite imagery to determine its reliability. The objective of this study was to investigate the feasibility of estimating FVC using different VIs (NDVI, SR, SAVI and MSAVI), calculated using radiometric information and Landsat 8 imagery, and to determine the differences that exist when estimating FCV with both sources of information. The radiometric information was collected in six corn plots located in the municipality of Texcoco, State of Mexico. The results showed a good fit of the VI calculated with field information when the FVC was less than 60 %. The correlation between the FVC measured in the field and the indices estimated with satellite imagery had R^2 values greater than 0.78, slightly higher in the case of the NDVI_L ($R^2 = 0.89$). This value suggests an acceptable degree of adjustment. It is concluded that estimating the FCV in a maize crop using spectral images from Landsat 8 is feasible. The best



fit between the field VI and the VI, calculated with Landsat 8 data for the conditions of this study, corresponded to the NDVI.

Keywords: Vegetation cover fraction (FCV), vegetation indices (IV), Landsat 8, radiometer, Canopeo.

Resumen

La fracción de cobertura vegetal (FCV) es una variable biofísica relacionada con la biomasa, el índice de área foliar y el coeficiente de cultivo, entre otros. Actualmente, con la amplia disponibilidad de imágenes satelitales, es posible estimar la FCV de forma extensiva usando índices de vegetación (IV). No obstante, es importante examinar la relación entre la FCV medida en campo y la estimada con imágenes satelitales para conocer su confiabilidad. El objetivo del presente estudio fue examinar la viabilidad de estimar la FCV utilizando diferentes IV (NDVI, SR, SAVI y MSAVI), calculados mediante información radiométrica e imágenes Landsat 8, y determinar las diferencias que existen al estimar la FCV con ambas fuentes de información. La información radiométrica se levantó en seis parcelas de maíz ubicadas en el municipio de Texcoco, Estado de México. Los resultados mostraron un buen ajuste de los IV calculados con información de campo cuando la FCV fue menor del 60 %. La correlación entre la FCV medida en campo y los índices estimados con imágenes satelitales tuvieron valores de R^2 superiores a 0.78, siendo ligeramente mayor en el caso del NDVI_L ($R^2 = 0.89$), valor que sugiere un grado aceptable de ajuste. Se concluye que es viable estimar la FCV en un cultivo de maíz empleando imágenes espectrales de Landsat 8. El



mejor ajuste entre los IV de campo y los IV calculados con datos de Landsat 8 para las condiciones de este estudio correspondió al NDVI.

Palabras clave: fracción de cobertura vegetal (FCV), índices de vegetación (IV), Landsat 8, radiómetro, Canopeo.

Received: 04/03/2021

Accepted: 27/03/2022

Introduction

In the field of remote sensing, the red (R) and near-infrared (NIR) bands of the electromagnetic spectrum are helpful in assessing the vigor of vegetation (Paz *et al.*, 2014), which is achieved by estimating biophysical variables from vegetation indices (VIs). According to Gilabert, González-Piqueras and García-Haro (1997), a VI is a value calculated from the relationship between reflectance measured at different wavelengths; these authors also point out that the R and NIR zones contain 90 % of vegetation data. A VI was first used by Jordan (1969), using the NIR: R ratio to derive the leaf area index. Subsequently, different VIs were developed and evaluated, namely the NDVI (Rouse, Hass, Schell, Deering, & Harlan, 1974), SAVI (Huete, 1988), and MSAVI (Qi, Chehbouni, Huete, Kerr, & Sorooshian, 1994), among others.

The biophysical variables useful for monitoring vegetation growth include fractional vegetation cover (FVC), defined by Song *et al.* (2017)



as the ratio of the vertical projection area of vegetation to the total surface area, generally expressed relative to a unit of area. According to Marcial, Ojeda, González and Jiménez (2017), FVC is directly related to vegetative growth and evapotranspiration because the evolution of plant cover affects the crop coefficient. In addition, using remote sensors to estimate biophysical variables significantly reduces the costs associated with field sampling (Paz, 2018), thus optimizing economic, personnel, and time resources. Hence the importance of obtaining accurate FVC estimates.

Software to measure FVC from digital photographs is currently available, as is the case of the Canopeo application developed by Patrignani and Oschner (2015). This tool uses the red/green (R/G), blue/green (B/G), and excess green (2G-R-B) ratios to determine if a pixel contains vegetation. However, since its use is limited to small areas, it is necessary to resort to satellite imagery when extensive areas require analysis.

Johnson and Trout (2012), working with different horticultural crops, obtained a strong correlation ($R^2 = 0.96$) between FVC and NDVI estimated with Landsat 5 satellite images. Similarly, Cuesta, Montoro, Jochum, López and Calera (2005) obtained a strong fit ($R^2 = 0.96$) by relating the FVC of several cultures to the NDVI estimated from Landsat 5 and Landsat 7 images. However, the areas analyzed by Johnson and Trout (2012) covered between 5 ha and 30 ha, while Cuesta *et al.* (2005) refer that the crop area analyzed in their study was larger than one hectare.

For this reason, it is necessary to assess whether using remote satellite-level sensors to estimate FVC is suitable for small maize plots of

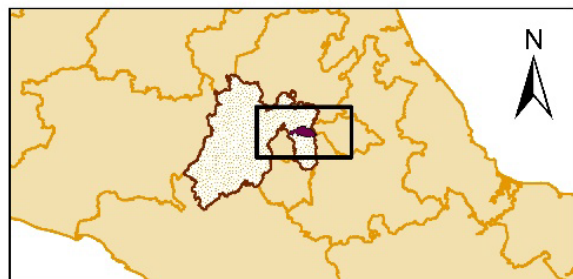


less than one hectare since few pixels with information are available in these cases. The present study compared the FVC of maize crops with four VIs estimated using remote sensor data recorded at the surface level and from Landsat 8 images. Afterward, field-measured FVC was contrasted with the Canopeo smartphone app using digital photographs. The objectives of this study were to validate the usefulness and accuracy of VIs for calculating FVC and demonstrate non-significant differences in accuracy between FVC estimated from satellite images and FVC measured in the field.

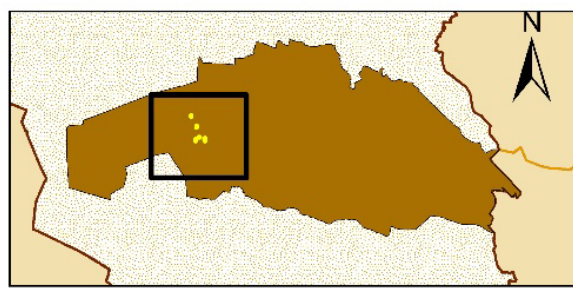
Study area

The study area is located in the municipality of Texcoco de Mora, State of Mexico, at an altitude of 2250 m a, characterized by a climate BS1 (dry semi-arid) and summer precipitation. Five rainfed and one irrigated maize plots were studied; in plot 3, irrigation was applied at the planting stage and again at seedling emergence. Cultural practices were managed according to the knowledge and experience of peasants. The location and data of the plots studied are shown in Figure 1.





Location of Texcoco, State of Mexico



Location of the plots studied

Plot	Area ha	Plant density per m ²	Field visits		
			Start date	Final date	Number of visits
1	0.9	4.6	31/05/2019	13/10/2019	13
2	1.0	6.0	31/05/2019	20/09/2019	13
3	1.1	6.5	15/06/2019	13/10/2019	13
4	1.2	8.0	28/06/2019	11/09/2019	11
5	0.9	4.9	27/05/2019	20/08/2019	11
6	0.9	6.1	27/05/2019	20/08/2019	11

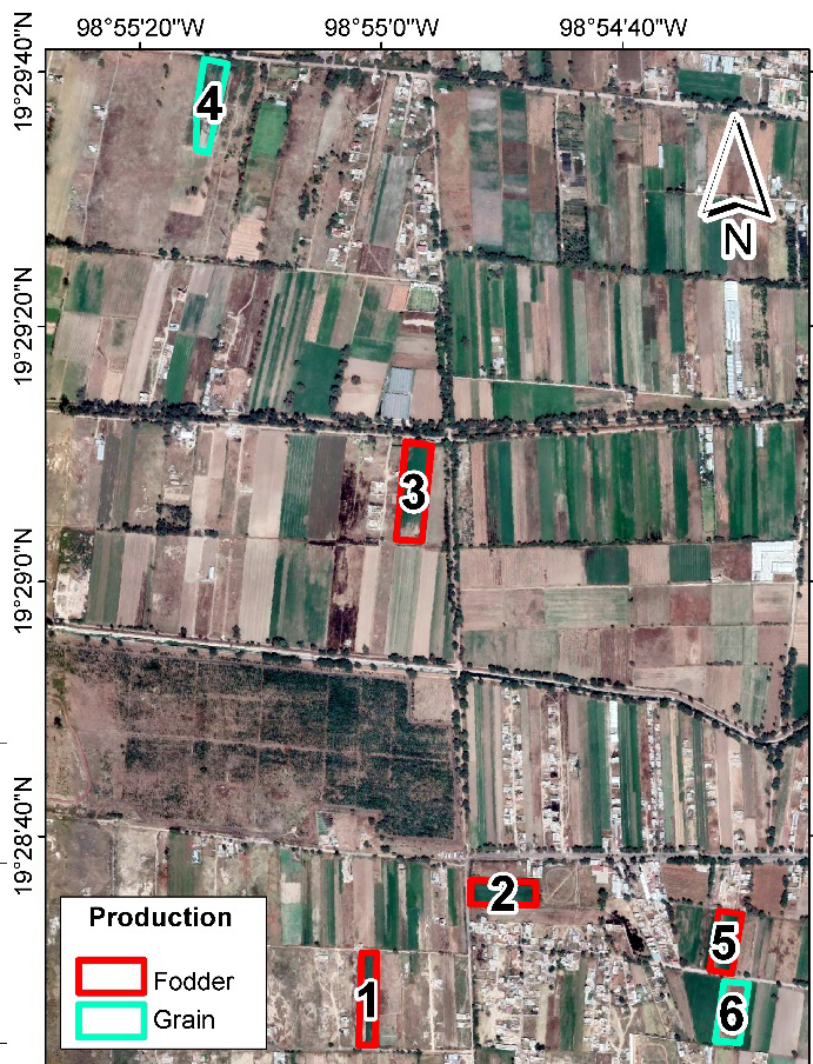


Figure 1. Location, plant density, field visits, and production objective of the plots studied.

Materials and methods

Radiometric information and digital photographs were recorded in parallel throughout the study. To this end, a 10 Mpx digital camera (SONY) and a multispectral radiometer (MSR, CropScan Inc.) were affixed to an extendable pole equipped with a bubble level to ensure data collection perpendicular to the canopy (a nadir) at 3 m height. The radiometer recorded data on five electromagnetic spectrum bands: blue (450–520 nm), green (520–600 nm), red (630–690 nm), near-infrared (760–900 nm), and mid-infrared (1550–1750 nm), and had double filters for each spectral band that simultaneously measured incident and reflected radiation. In addition, the radiometer data acquisition and calibration software facilitated the analog-to-digital conversion of voltage and recorded reflectance in the five spectral bands for each data set.

Field data were recorded between 10:00 h and 14:00 h (local time) to avoid wide variations in the solar zenith angle. Seventeen sampling points arranged following a zigzag pattern were selected within plots (Figure 2), which differed in each field visit. At each sampling point, one photograph and three reflectance readings were taken and averaged to obtain the measured reflectance value.



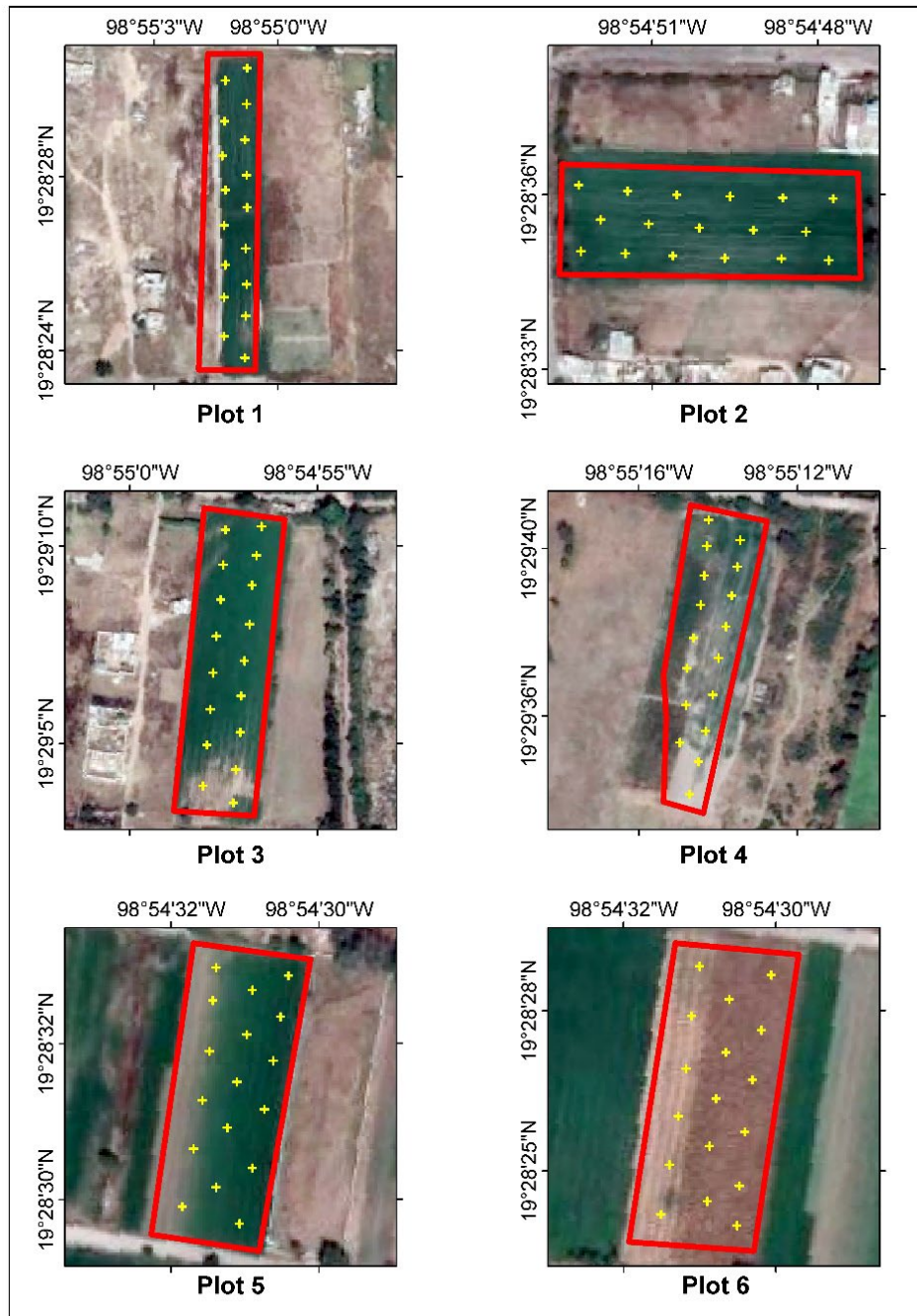


Figure 2. Individual location and diagram of field data recording in each plot.

During the study period, seven Landsat 8 images were obtained, showing a cloud cover between 0 % and 70 %; although some of these images had a high cloud cover, the area on the evaluated plots was free of clouds, making them suitable for use. These images capture reflectance data in 11 wavelength bands of the electromagnetic spectrum, divided into Operational Land Imager (OLI) and Thermal Infrared Sensor (TIRS) bands. These images were downloaded from the United States Geological Survey (USGS) website (<https://earthexplorer.usgs.gov/>) with processing level L1TP (with radiometric calibration and orthorectification) and no atmospheric correction.

The effect of the atmosphere was corrected with the QGIS software version 3.8.2. To this end, we used the Semi-Automatic Classification Plugin (SCP), which is based on the dark object subtraction technique (Chavez, 1996). Then, the plots' polygons were defined using Google Earth to extract reflectance data corresponding to band 4 (red) and band 5 (near-infrared) using QGIS.

Field radiometric information and Landsat 8 images were used to estimate the following VIs: Simple Ratio (SR), Normalized Difference Vegetation Index (NDVI), Soil-Adjusted Vegetation Index (SAVI), and Modified Soil-Adjusted Vegetation Index (MSAVI). These indices were calculated using the equations shown in Table 1. On the other hand, FVC was measured with the Canopeo application for smartphones developed by Patrignani and Ochsner (2015) using digital photographs.



Table 1. Vegetation indices and Landsat 8 bands used for VI estimates.

Index	Equation	Bands	Source
SR*	$\frac{\text{NIR}_{783}}{\text{R}_{665}}$	B4 and B5	Jordan, 1969
NDVI**	$\frac{\text{NIR}_{783} - \text{R}_{665}}{\text{NIR}_{783} + \text{R}_{665}}$	B4 and B5	Rouse <i>et al.</i> , 1974
SAVI†	$\frac{\text{NIR}_{783} - \text{R}_{665}}{\text{NIR}_{783} + \text{R}_{665} + L} (1 + L)$	B4 and B5	Huete, 1988
MSAVI‡‡	$\frac{(2\text{NIR}_{783} + 1) - \sqrt{(2\text{NIR}_{783} + 1)^2 - 8(\text{NIR}_{783} - \text{R}_{665})}}{2}$	B4 and B5	Qi <i>et al.</i> , 1994

* Simple Ratio

**Normalized Difference Vegetation Index

†Soil-Adjusted Vegetation Index

‡‡Modified Soil-Adjusted Vegetation Index

The FVC measured *in situ* was first correlated with the VIs calculated from radiometer-measured reflectance. To this end, a double segmentation of the regression line was performed. The data set describing the first biophysical straight lines ranged from 0 % to 60 % FVC. For the subsequent line, FVC values greater than 60 % were used.

The FVC was then estimated using the VIs calculated with Landsat 8 images and compared with the FVC measured in the field using the Canopeo app.; this was done by averaging the FVC and VI values of the different plots. The values of these VIs for the date when field data were recorded were estimated from a simple linear interpolation. Finally, we



compared the VIs obtained with radiometric data versus those estimated using satellite images.

To avoid confusion in the terminology used, VIs estimated with radiometric information are identified with the subscript R (SR_R , $NDVI_R$, $SAVI_R$, and $MSAVI_R$) to distinguish them from VIs calculated using Landsat 8 images, which are denoted with the subscript L (SR_L , $NDVI_L$, $SAVI_L$, and $MSAVI_L$).

Statistical analysis

Two statistical efficiency parameters were used: the coefficient of determination (R^2), which indicates the ability of a model to replicate its results (Equation (1)), and the root mean square error (RMSE), which measures the variation of the calculated values relative to the observed values (Equation (2)):

$$R^2 = \frac{\sum_{i=1}^n (y_i - \bar{y})(\hat{y}_i - \bar{y}_i)}{\sqrt{\sum_{i=1}^n (y_i - \bar{y})^2 \sum_{i=1}^n (\hat{y}_i - \bar{y}_i)^2}} \quad (1)$$

$$RMSE = \sqrt{\frac{1}{n} \sum_{i=1}^n (\hat{y}_i - y_i)^2} \quad (2)$$

Where \bar{y}_i is the mean of the estimated data, \hat{y}_i is the estimated data, \bar{y} is the mean of the observed data, and y_i is the observed data.



Results

First, SR_R was correlated with FVC (Figure 3). This VI, within the FVC range of 0 % to 60 %, showed R^2 values between 0.60 and 0.80. For FVC data above 60 %, R^2 decreased to 0.30 for plot 1. On the other hand, the RMSE for FVC values up to 60 % ranged between 0.78 and 2.83 SR_R units. In contrast, for FVC values above 60 %, RMSE values varied between 1.50 and 2.79 SR_R units. For FVC values lower than or equal to 60 %, plot 5 had the lowest R^2 and the highest RMSE. These results were attributed to the fact that, when field sampling (Stage V7) started, maize plants had already attained an FVC close to 60 %. On the other hand, the highest R^2 values were recorded in plots 4 and 6, which were evaluated over the whole crop cycle.



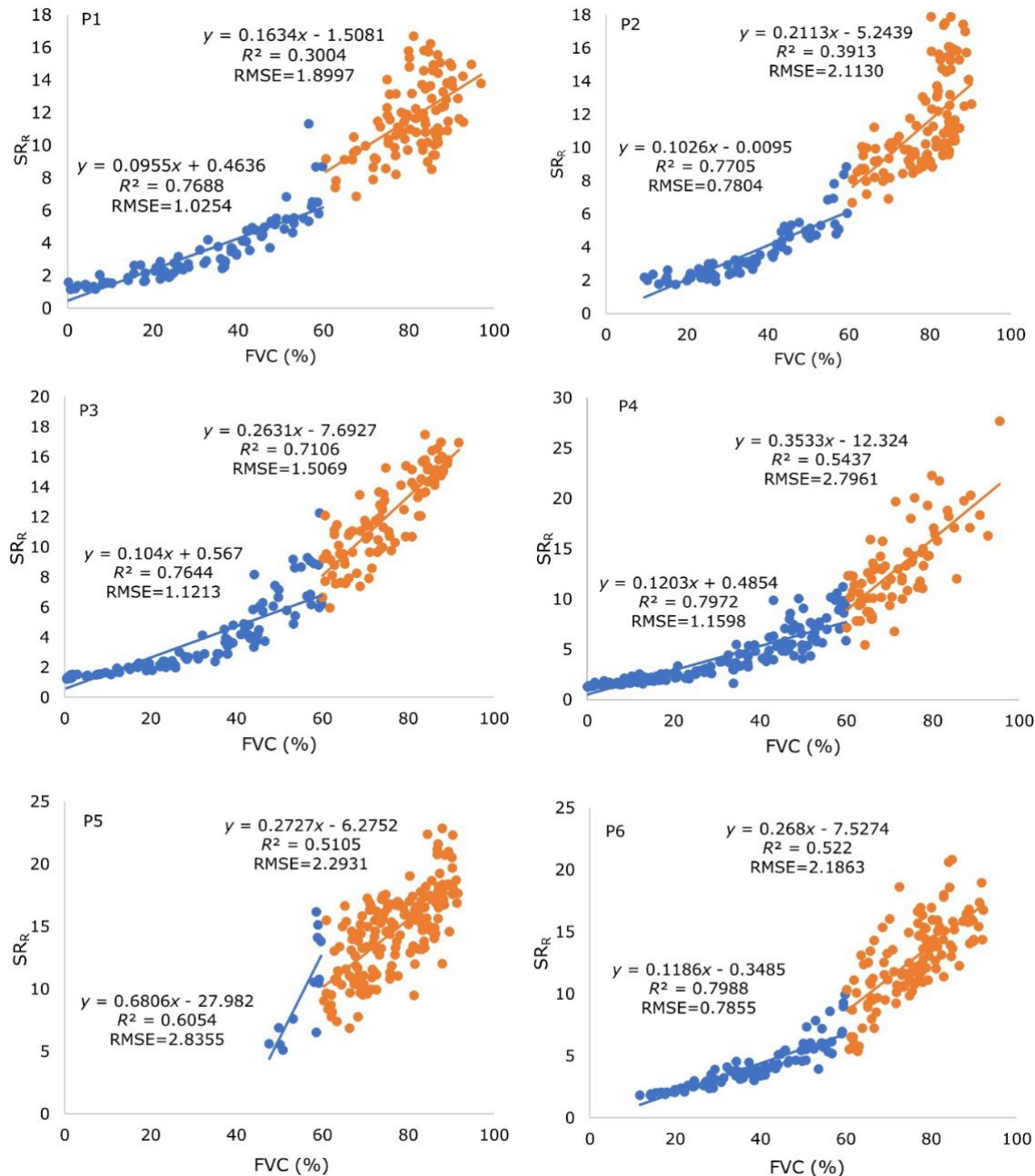


Figure 3. Relationship between FVC measured with the Canopeo application and SR_R estimated with radiometric data in the six plots studied.

The following VI analyzed was NDVI_R (Figure 4). The R^2 values obtained indicate that NDVI_R attained a better fit with FVC than SR_R. Likewise, the low RMSE values suggest a minimal overestimation of FVC. For FVC values up to 60 %, plot 3 showed the best fit ($R^2 = 0.96$) and plot 5 had the lowest fit ($R^2 = 0.70$); this situation is likely because a field visit to plot 5 occurred when the crop had an FVC lower than 60 %. On the other hand, R^2 values for FVC above 60 % ranged between 0.34 and 0.63 and were lower than those obtained with the SR_R. In this regard, Campos, Neale, López, Balbontín and Calera (2014) reported an R^2 of 0.93 when the FVC of vineyards was related to the NDVI estimated using Landsat 5 TM images. The R^2 calculated by these authors is similar to the value obtained in the present study.

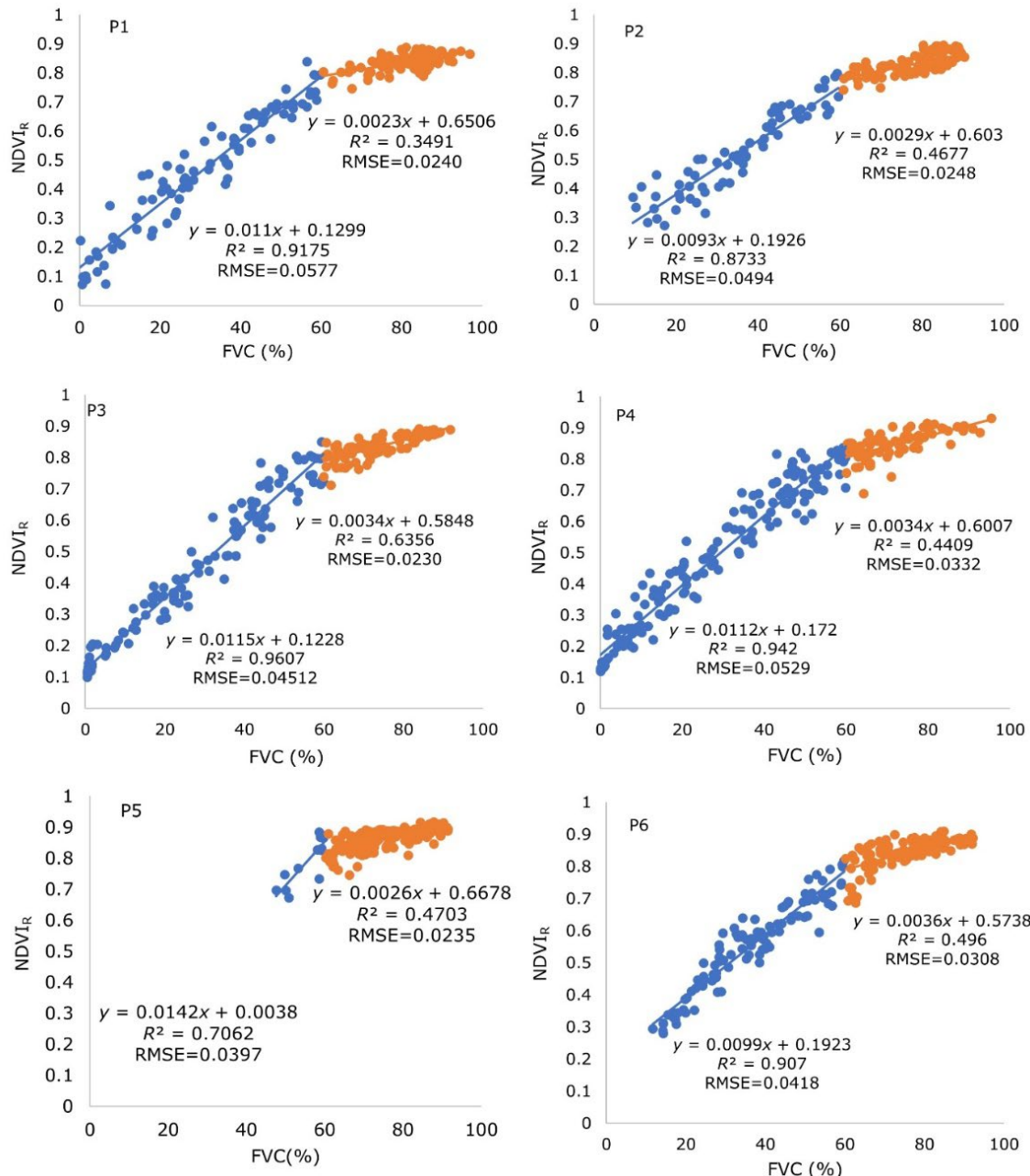


Figure 4. Relationship between FVC measured with the Canopeo application and NDVI_R estimated with radiometric data in the six plots studied.

According to Aparicio, Villegas, Casadesus, Araus and Royo (2000), the lower R^2 values observed when FVC exceeds 60 % are explained by the saturation of reflectance in the red band, a phenomenon that turns NDVI insensitive to plant covers above 60 %. On the other hand, Purevdorj, Tateish, Ishiyama and Honda (1998), conducting a study in grasslands using NDVI, point out that leaf overlap leads to great errors when estimating FVC. In grasslands, these authors found that the error in FVC estimates increases when FVC values exceed 40 %. According to Schlemmer *et al.* (2013), the absorption coefficient of chlorophyll in the red band is high, so when chlorophyll content reaches 0.8 g m^{-2} , which occurs for leaf area index (LAI) values close to 2.0, red-band reflectance becomes saturated. Thus, NDVI increases linearly in the early growth stages and becomes asymptotic as LAI increases (De-la-Casa, Ovando, Ravelo, Abril, & Bergamaschi, 2014; Jiang *et al.*, 2006).

Figure 5 shows the correlation between FVC and SAVI_R for each plot evaluated. Again, the highest R^2 correspond to FVC values lower than or equal to 60 %, ranging from 0.71 to 0.96. These R^2 values are similar to those obtained by Campos *et al.* (2014), who reported an R^2 of 0.91 when grapevine FVC was related to the SAVI estimated using Landsat 5 TM images. In contrast, R^2 values decreased for FVC higher than 60 % (0.36 to 0.65). According to Venancio *et al.* (2019), SAVI is a suitable estimator of FVC because it includes a correction factor to account for soil exposure. However, we observed that FVC data above 60 % follow the same asymptotic trend as NDVI_R . This behavior is because the SAVI was created from the NDVI to minimize the influence of solar geometry, visualization geometry, soil background, and atmospheric effects (Rondeaux, Steven, & Baret, 1996). However, it has the same constraints as the NDVI because the R-band becomes rapidly saturated.

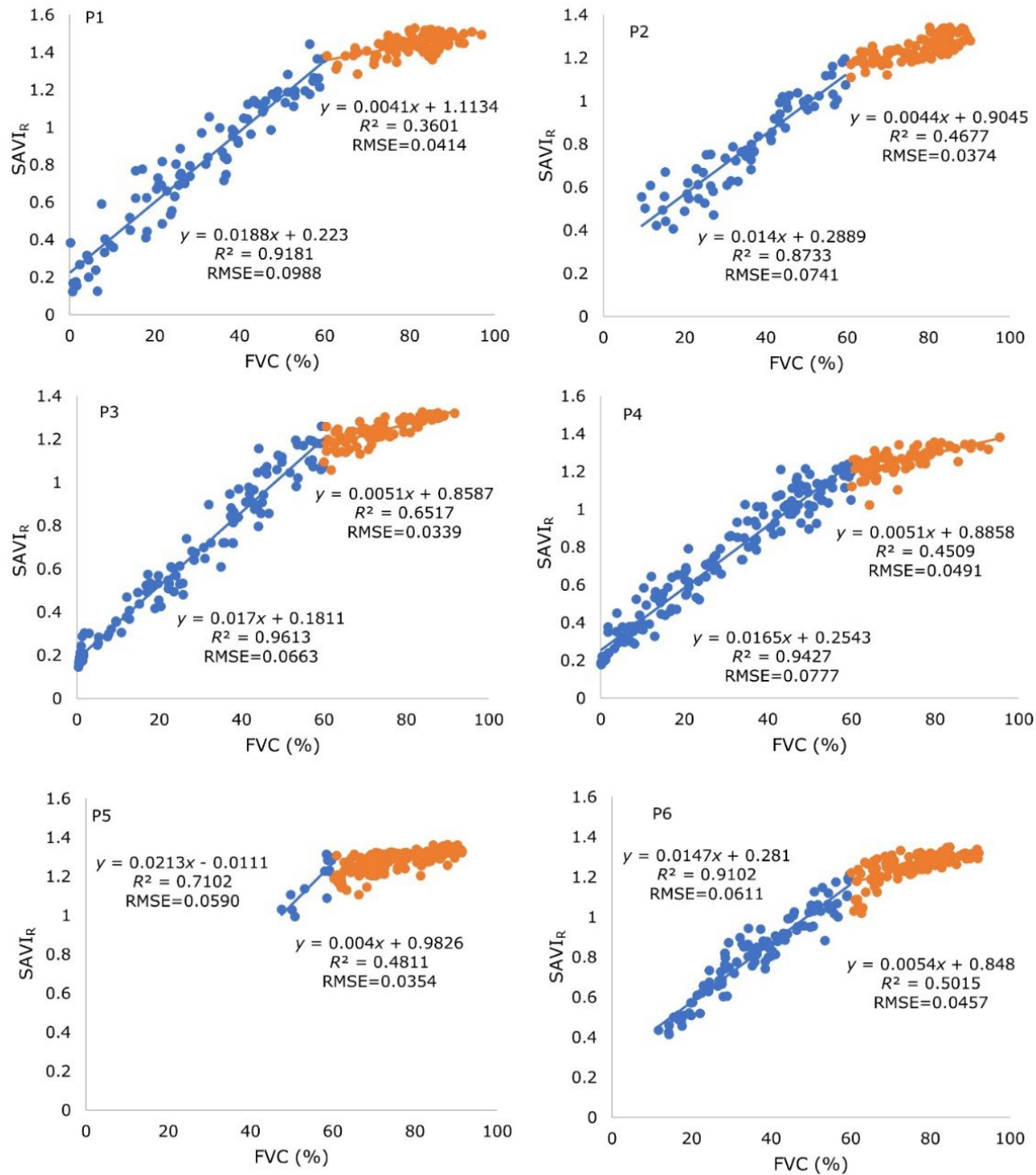


Figure 5. Relationship between FVC measured with the Canopeo application and SAVI_R estimated with radiometric data in the six plots studied.

As regards the RMSE, the highest values were obtained when the FVC was lower than 60 %. This finding is attributed to the greater data dispersion at this stage, probably due to the greater influence of the soil background on the reflectance values recorded, and because we used a fixed value as the soil brightness correction factor ($L = 0.5$) recommended for intermediate plant cover conditions (Huete, 1988). In contrast, RMSE was lower for FVC values higher than 60 %, indicating less variability at this stage because of the minimum effect of soil reflectance and its variability (humidity, color, etc.) (Paz, 2018).

Figure 6 shows the correlation between FVC and MSAVI_R. MSAVI is a modification of the SAVI to expand the dynamic range of the vegetation signal while minimizing the optical influence of the soil background (Jiang *et al.*, 2006). R^2 was higher for FVC values below 60 %, ranging from 0.71 to 0.95, and lower for FVC values above 60 %. In this sense, when different VIs were related to FVC in grasslands, Purevdorj *et al.* (1998) obtained R^2 values of 0.92, 0.89, and 0.89 for NDVI, SAVI, and MSAVI, respectively. With respect to MSAVI_R, R^2 values were higher for plots 3 and 4 and similar for plots 1, 2, and 6. On the other hand, the lowest RMSE values were obtained when FVC was higher than 60 % associated with the asymptotic trend, which causes a lower MSAVI_R variability.

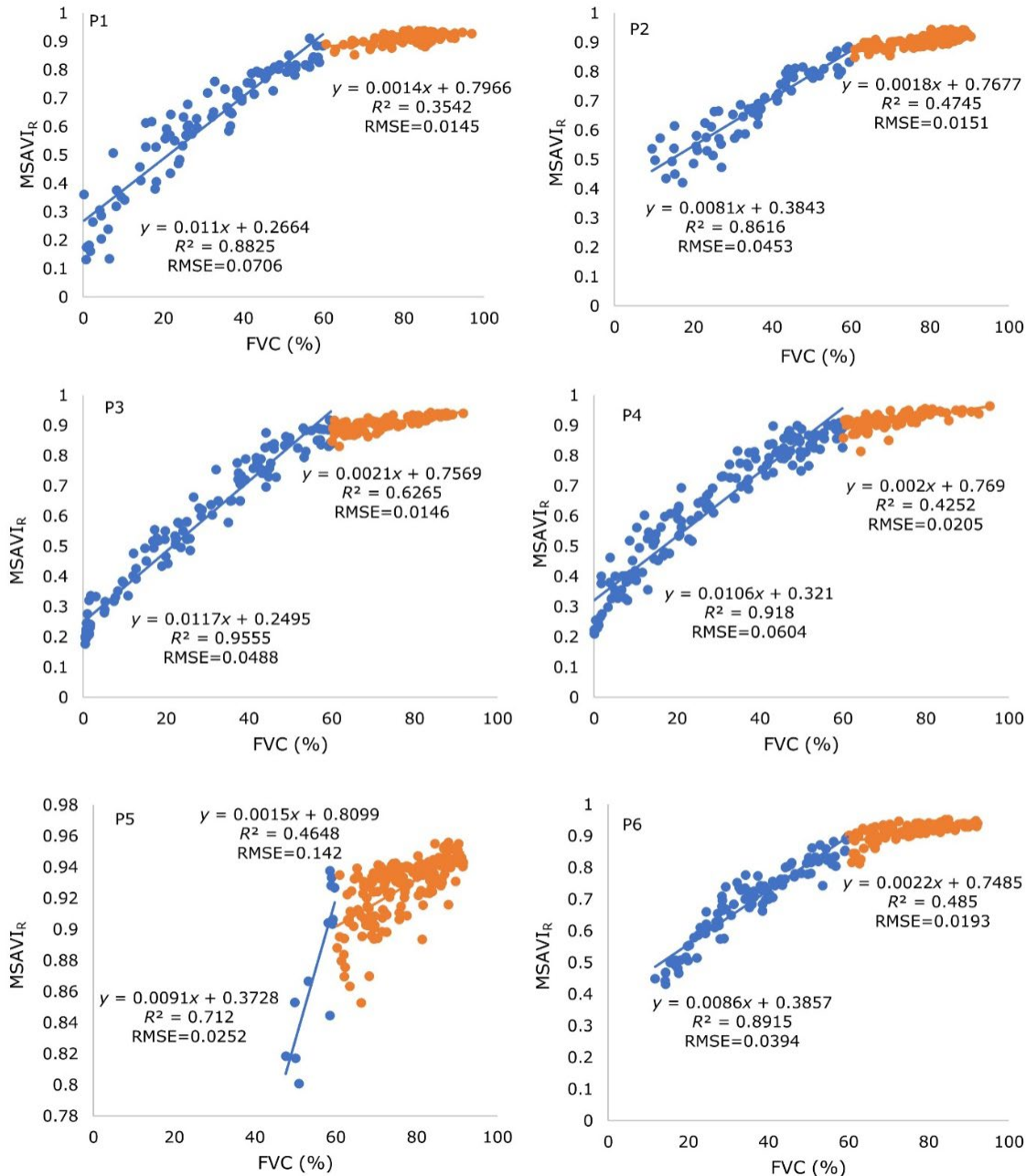


Figure 6. Relationship between FVC measured with the Canopeo application and MSAVI_R estimated with radiometric data in the six plots studied.

The comparisons between the VIs estimated from Landsat 8 images and the FVC measured with the Canopeo application are shown in Figure 7. It shows an R^2 greater than 0.86 between field-measured FVC and VI data estimated with satellite imagery, except for the SR_L index, which had a fit (R^2) of 0.78. In general, the results obtained by comparing field-measured FVC with the trend of the indices estimated from satellite imagery yielded satisfactory estimates, with $NDVI_L$ being the index with the best fit ($R^2 = 0.89$). These data are consistent with those by De-la-Casa *et al.* (2014), who reported R^2 values of 0.875 and 0.864 using the indices NDVI and SAVI, respectively, when making the same comparisons for maize plots under different soil moisture conditions. Using Prova-V images (100 m spatial resolution), De-la-Casa *et al.* (2018) obtained an R^2 of 0.94 for NDVI, higher than the value reported in Figure 5. By contrast, using HJ-1A/B images with a 30 m spatial resolution, Jin *et al.* (2017) reported an R^2 of 0.58 when the wheat FVC was related to the Modified Triangular Vegetation Index 2 (MTVI2). The result obtained by these authors was lower than the R^2 value observed in the present study since the lowest fit with SR_L was 0.78.



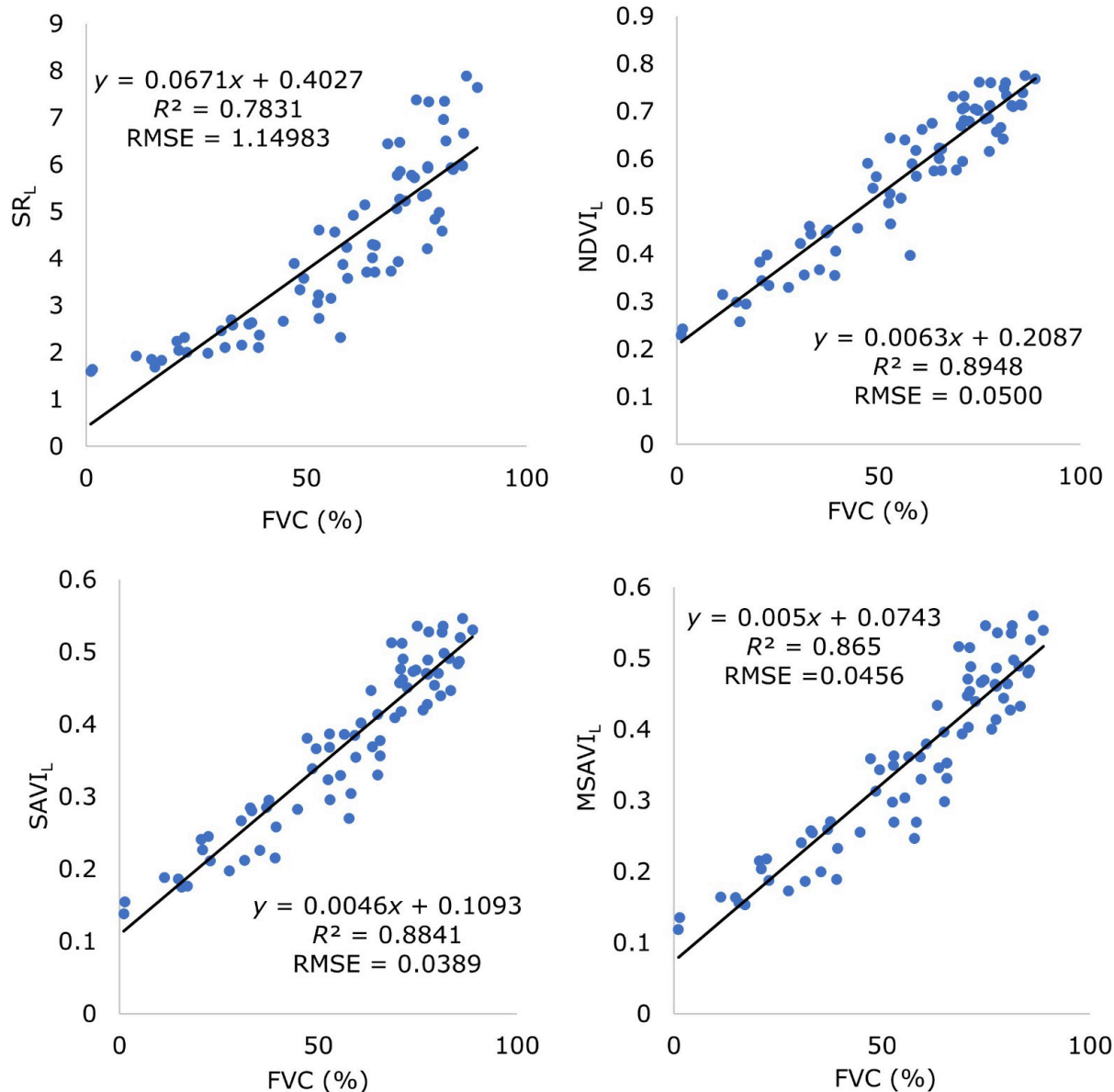


Figure 7. Correlations between field-measured FVC and VIs estimated from Landsat 8 images.

Figure 8 shows the correlation between the VIs estimated with radiometric field data and VIs estimated with Landsat 8 images. A high correlation is observed between the average VIs estimated with Landsat 8 images and the VIs estimated with radiometric field data for the four indices analyzed ($R^2 > 0.96$), thus confirming the high reliability of these indices when used for estimating FVC. Paz (2018) mentions that VIs have been used to estimate FVC, with NDVI being the index most studied and compared with radiation simulations and field measurements. The large dispersion in the correlations is due to the variation in the optical properties of leaves and their angular distribution. The best fit (highest R^2 and lowest RMSE) between field VIs and VIs estimated with Landsat 8 data was NDVI.



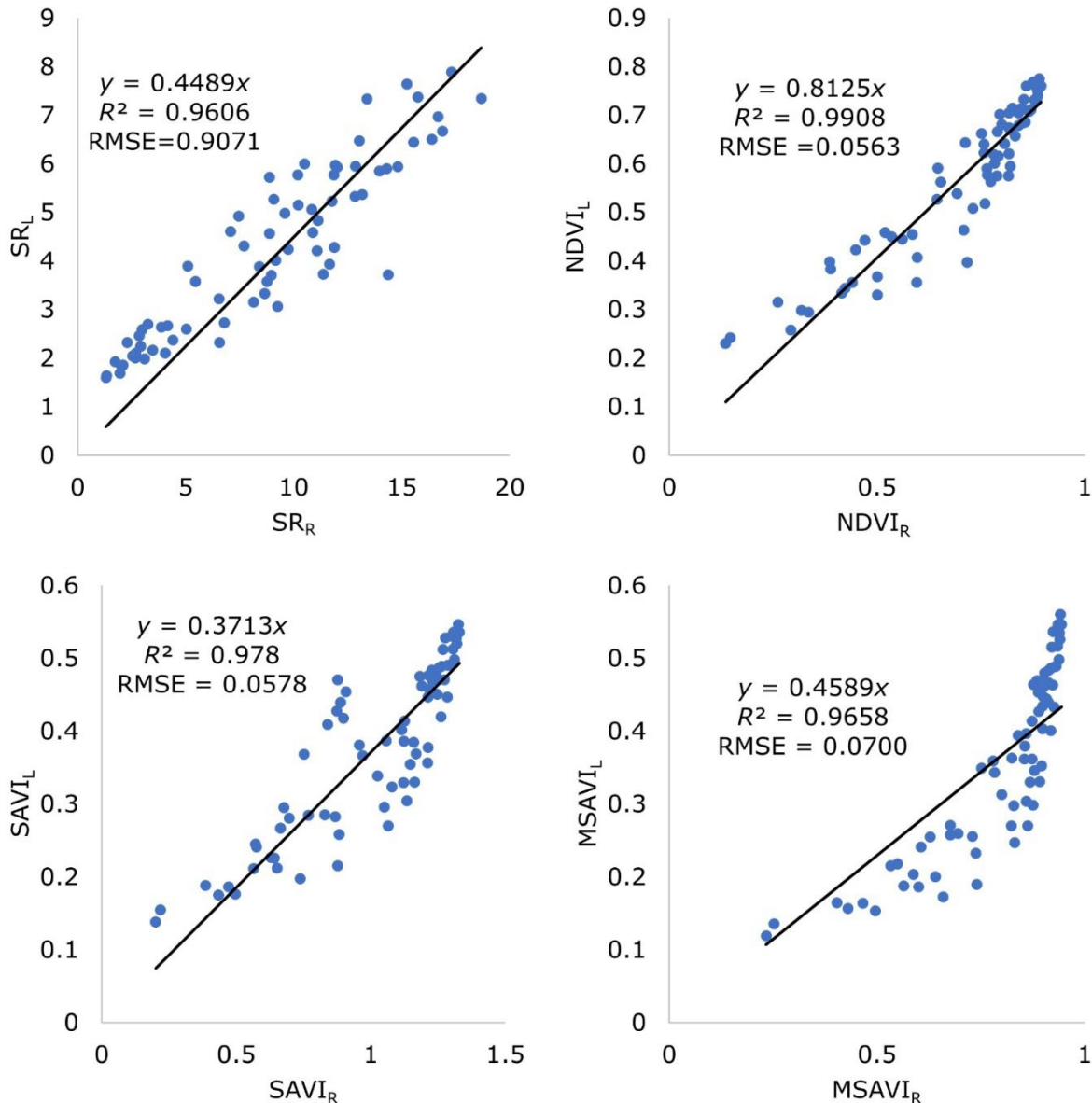


Figure 8. Correlation between VIs obtained with radiometer data and VIs estimated with Landsat 8 images.

Discussion

The high RMSE values obtained for SR indicate that this VI may lead to highly overestimated FVC values despite the high R^2 . According to Pinty and Verstraete (1992), atmospheric components tend to reduce the SR, and their spatial and temporal variability makes atmospheric corrections even more necessary and hard to apply in the field. Despite the constraints of the SR, Aparicio *et al.* (2000) related it to the yield of different wheat genotypes, finding that this VI showed a better correlation than NDVI with crop growth under rainfed conditions.

In this sense, Bocco, Ovando, Sayago and Willington (2013) developed a model based on SR to estimate FVC in soybean and maize crops using MODIS-AQUA images. These authors obtained R^2 values of 0.68 with a linear model and 0.89 with an exponential model. In the case of the linear model, the R^2 obtained for FVC values lower than 60 % in the present study are higher than the R^2 reported by these authors. These differences may be related to the size of the study area since Bocco *et al.* (2013) used plots of approximately 50 ha, while this study was conducted on plots of about 1 ha, which were highly heterogeneous partly due to soil salinity and scarce rainfall.

The results of the relationship between NDVI and FVC were similar to those obtained by De-la-Casa *et al.* (2014), who reported an R^2 of 0.87 when evaluating models for estimating maize FVC from MODIS-AQUA data, as well as an RMSE of 9.8 %, higher than the value obtained in this study. On the other hand, Bocco *et al.* (2013), estimating FVC with the



NDVI and applying a linear model, obtained an RMSE of 11.7 % and an R^2 of 0.76; the latter is lower than values obtained when FVC was below 60 %. The differences between the findings reported by these authors and the present study may be related to the fact that their images had a 250 m spatial resolution in the R and NIR bands. On the other hand, Zhang, Smith and Hill (2011), estimating FVC from digital photographs of grasslands in Canada using a linear relationship and the NDVI calculated from Landsat 5 TM images, obtained an R^2 of 0.55, lower than the value estimated in the present study.

Regarding the SAVI, the R^2 and RMSE values obtained in the present study are consistent with those reported by Bocco *et al.* (2013), with an R^2 of 0.83. Also, using the SAVI to estimate FVC, De-la-Casa *et al.* (2014) obtained an R^2 of 0.86 and an RMSE of 10.2 %, similar to those estimated in the present study. According to Venancio *et al.* (2019), the lowest SAVI ranges from 0.12 to 0.20, depending on soil type and agricultural practices, while maximum values range from 0.68 to 0.70. On the other hand, Huete (1988) mentions that the SAVI should range from 0 to 1. However, in this study, values above 1.3 were found in all plots; this is related to the algebraic bases of the SAVI, which include an optimal adjustment factor to reduce noise from the soil background on the plant canopy (Huete, 1988; Rondeaux *et al.*, 1996; Ren, Zhou, & Zhang, 2018; Venancio *et al.*, 2019). Thus, the highest SAVI values found in the present study are attributed to using a constant L throughout the crop cycle.

Separately, Bocco *et al.* (2013) reported an R^2 of 0.83 between MSAVI and FVC, and an RMSE of 10.3 %, similar to the value obtained in

this study, while Chen *et al.* (2019), relating FVC to MSAVI, found an R^2 of 0.77 and an RMSE of 7.8 % using a linear model. These findings show that the relationship between MSAVI and the R and NIR spectral bands under field conditions exceeds the relationship proposed by Chen *et al.* (2019). This discrepancy may be due to the resolution of the images used.

Despite the adequate relationship between FVC and the VIs analyzed, Paz *et al.* (2015) point out that most VIs have design constraints. These authors found that linear VIs are equivalent to each other, a behavior confirmed for the indexes analyzed in the present study. Furthermore, they point out that a VI yielding better results than another depends on the particular case studied and the acceptance criteria used; therefore, these methodologies should be used cautiously.

Conclusions

The best fit of the vegetation indices evaluated in this study with field information was observed for fractional vegetation cover values lower than 60 %. When these values exceed 60 %, we observed an asymptotic effect of these indices due to the saturation of the red spectral band. The best fit (highest R^2 and lowest RMSE) between the vegetation indices calculated with field radiometric data and those estimated with Landsat 8 image data was achieved with the NDVI.

Comparing the field-measured fractional vegetation cover against the vegetation indices estimated with Landsat 8 images resulted in a coefficient of determination higher than 0.78 in all plots. This strong



correlation is attributed to the high relationship between the vegetation indices estimated from field radiometric information and those derived from satellite image data. These results confirm that variables such as the fractional vegetation cover can be accurately estimated using Landsat 8 images, even in small maize plots with areas of around one hectare.

Acknowledgments

To the Consejo Nacional de Ciencia y Tecnología (Conacyt) for the grant awarded to José Miguel Muñoz Pérez to undertake the M. Sc. Studies. María Elena Sánchez-Salazar translated the manuscript into English.

References

- Aparicio, N., Villegas, D., Casadesus, J., Araus, J. L., & Royo, C. (2000). Spectral vegetation indices as nondestructive tools for determining durum wheat yield. *Agronomy Journal*, 92(1), 83-91. DOI: <https://doi.org/10.2134/agronj2000.92183x>
- Bocco, M., Ovando, G., Sayago, S., & Willington, E. (2013). Simple models to estimate soybean and corn percent ground cover with vegetation indices from modis. *Revista de Teledetección*, 39(39), 83-91.



Campos, I., Neale, C. M. U., López, M. L., Balbontín, C., & Calera, A. (2014). Analyzing the effect of shadow on the relationship between ground cover and vegetation indices by using spectral mixture and radiative transfer models. *Journal of Applied Remote Sensing*, 8(083562), 1-21. DOI: 10.1117/1.JRS.8.083562

Chavez, P. S. (1996). Image-based atmospheric corrections-revisited and improved. *Photogrammetric engineering and remote sensing*, 62(9), 1025-1035.

Chen, X., Guo, Z., Chen, J., Yang, W., Yao, Y., Zhang, C., Cui, X., & Cao, X. (2019). Replacing the Red Band with the Red-SWIR Band ($0.74\rho_{\text{red}} + 0.26\rho_{\text{swir}}$) can reduce the sensitivity of vegetation indices to soil background. *Remote Sensing*, 11(7), 851. DOI: <https://doi.org/10.3390/rs11070851>

Cuesta, A., Montoro, A., Jochum, A. M., López, P., & Calera, A. (2005). Metodología operativa para la obtención del coeficiente de cultivo desde imágenes satelitales. *ITEA*, 101, 212-224.

De-la-Casa, A. C., Ovando, G. G., Ravelo, A. C., Abril, E. G., & Bergamaschi, H. (2014). Estimating maize ground cover using spectral data from Aqua-MODIS in Córdoba, Argentina. *International Journal of Remote Sensing*, 35(4), 1295-1308. DOI: 10.1080/01431161.2013.876119

De-la-Casa, A., Ovando, G., Bressanini, L., Martínez, J., Díaz, G., & Miranda, C. (2018). Soybean crop coverage estimation from NDVI images with different spatial resolution to evaluate yield variability in a plot. *ISPRS Journal of Photogrammetry and Remote Sensing*, 146, 531-547. DOI: <https://doi.org/10.1016/j.isprsjprs.2018.10.018>

Gilabert, M., González-Piqueras, J., & García-Haro, J. (1997). Acerca de los índices de vegetación. *Revista de Teledetección*, 8. Recovered from https://www.researchgate.net/publication/39195330_Acerca_de_los_indices_de_vegetacion/link/00b7d5187635eb5a1a000000/download

Huete, A. (1988). A soil-adjusted vegetation index (SAVI). *Remote Sensing of Environment*, 25(295-309). Recovered from [https://doi.org/10.1016/0034-4257\(88\)90106-X](https://doi.org/10.1016/0034-4257(88)90106-X)

Jiang, Z., Huete, A. R., Chen, J., Chen, Y., Li, J., Yan, G., & Zhang, X. (2006). Analysis of NDVI and scaled difference vegetation index retrievals of vegetation fraction. *Remote Sensing of Environment*, 101(3), 366-378. DOI: <https://doi.org/10.1016/j.rse.2006.01.003>

Jin, X., Li, Z., Yang, G., Yang, H., Feng, H., Xu, X., Wang, J., Li, X., & Luo, J. (2017). Winter wheat yield estimation base on multi-source medium resolution optican and radar imaging data and AquaCrop model using the particle swarm optimization algorithm. *ISPRS Journal of Photogrammetry and Remote Sensing*, 126, 24-37. DOI: <https://doi.org/10.1016/j.isprsjprs.2017.02.001>



Johnson, L. F., & Trout. T. J. (2012). Satellite NDVI assisted monitoring of vegetable crop evapotranspiration in California's San Joaquin Valley. *Remote Sensing*, 4(2), 439-455. DOI: <https://doi.org/10.3390/rs4020439>.

Jordan, C. F. (1969). Derivation of leaf-area index from quality of light on the forest floor. *Ecology*, 50(4), 663-666. DOI: <https://doi.org/10.2307/1936256>

Marcial, M. J., Ojeda, W., González, A., & Jiménez, S. (2017). *Estimación de la cobertura vegetal usando imágenes RGB obtenidas desde un dron*. III Congreso Nacional de riego y drenaje COMEII 2017, COMEI-17048.

Patrignani, A., & Ochsner, T. E. (2015). Canopeo: A powerful new tool for measuring fractional green canopy cover. *Agronomy Journal*, 107(6), 2312-2320. DOI: <https://doi.org/10.2134/agronj15.0150>

Paz, F. (2018). Estimación de la cobertura aérea de la vegetación herbácea usando sensores remotos. *Terra Latinoamericana*, 36(3), 239-259. DOI: <https://doi.org/10.28940/terra.v36i3.399>

Paz, F., Romero, M. E., Palacios, E., Bolaños, M., Valdez, J. R., & Aldrete, A. (2014). Alcances y limitaciones de los índices espectrales de la vegetación: marco teórico. *Terra Latinoamericana*, 32(3), 177-194. Recovered from <https://www.terralatinoamericana.org.mx/index.php/terra/article/view/22/20>

Paz, F., Romero, M., Palacios, E., Bolaños, M., Valdez, J., & Aldrete, A. (2015). Alcances y limitaciones de los índices espectrales de la vegetación: análisis de índices de banda ancha. *Terra Latinoamericana*, 33, 27-49. Recovered from <http://www.scielo.org.mx/pdf/tl/v33n1/2395-8030-tl-33-01-00027.pdf>

Pinty, B., & Verstraete, M. M. (1992). GEMI: A non-linear index to monitor global vegetation from satellites. *Vegetation*, 101, 15-20. DOI: <https://doi.org/10.1007/BF00031911>

Purevdorj, T., Tateish, R., Ishiyama, T., & Honda, Y. (1998). Relationships between percent vegetation cover and vegetation indices. *International Journal Remote Sensing*, 19(18), 3519-3535. DOI: <https://doi.org/10.1080/014311698213795>

Qi, J., Chehbouni, A., Huete, A., Kerr, Y., & Sorooshian, S. (1994). A Modified soil adjusted vegetation index. *Remote Sensing of Environment*, 48, 119-126. DOI: [https://doi.org/10.1016/0034-4257\(94\)90134-1](https://doi.org/10.1016/0034-4257(94)90134-1)

Ren, H., Zhou, G., & Zhang, F. (2018). Using negative soil adjustment factor in soil-adjusted vegetation index (SAVI) for aboveground living biomass estimation in arid grasslands. *Remote Sensing of Environment*, 209, 439-445. DOI: <https://doi.org/10.1016/j.rse.2018.02.068>

Rondeaux, G., Steven, M., & Baret, F. (1996). Optimization of soil-adjusted vegetation indices. *Remote Sensing of Environment*, 55(2), 95-107. DOI: [10.1016/0034-4257\(95\)00186-7](https://doi.org/10.1016/0034-4257(95)00186-7)



Rouse, J. W., Hass, R. H., Schell, J. A., Deering, D. W., & Harlan, J. C. (1974). *Monitoring the vernal advancement and retrogradation (greenwave effect) of natural vegetation*. NASA/GSFC, Type III, Final report, Greenbelt, MD. (pp. 1-390). Recovered from <https://ntrs.nasa.gov/api/citations/19750020419/downloads/19750020419.pdf>

Schlemmer, M., Gitelson, A., Schepers, J., Ferguson, R., Peng, Y., Shanahan, J., & Rundquist, D. (2013). Remote estimation of nitrogen and chlorophyll contents in maize at leaf and canopy levels. *International Journal of Applied Earth Observation and Geoinformation*, 25, 47-54. DOI: <https://doi.org/10.1016/j.jag.2013.04.003>

Song, W., Mu, X., Ruan, G., Gao, Z., Li, L., & Yan, G. (2017). Estimating fractional vegetation cover and the vegetation index of bare soil and highly dense vegetation with a physically based method. *International Journal of Applied Earth Observation and Geoinformation*, 58, 168-176. DOI: <https://doi.org/10.1016/j.jag.2017.01.015>

Venancio, L. P., Mantovani, E. C., Amaral, C. H., Neale, C. M. U., Gonçalves, I. Z., Filgueiras, R., & Campos, I. (2019). Forecasting corn yield at the farm level in Brazil based on the FAO-66 approach and soil-adjusted vegetation index (SAVI). *Agricultural Water Management*, 225 (105779). DOI: <http://doi.org/10.1016/j.agwat.2019.105779>

Zhang, Y., Smith, A. M., & Hill, M. J. (2011). Estimating fractional cover of grassland components from two satellite remote sensing sensors. *Proceedings of 34th International Symposium on Remote Sensing of Environment* (pp. 10-15). Sydney, Australia. Recovered from <https://www.isprs.org/proceedings/2011/isrse-34/211104015Final00252.pdf>